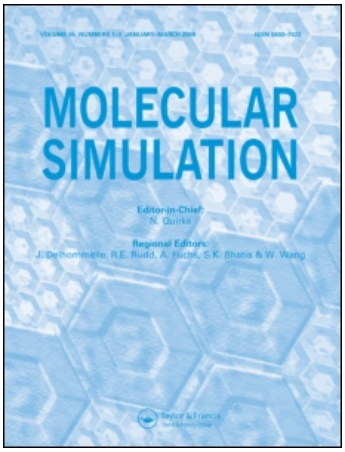

Molecular Simulation
Publication details, including instructions for authors and subscription information:
http://www.informaworld.com/smpp/title~content=t713644482

Molecular Dynamics Simulation Studies of the Limiting Conductances of $MgCl_2$ and $CaCl_2$ in Supercritical Water Using SPC/E Model for Water

Geun Hoi Goo[a]; Gihong Sung[a]; Song Hi Lee[a]
[a] Department of Chemistry, Kyungsung University, Busan, South Korea

To cite this Article Goo, Geun Hoi , Sung, Gihong and Lee, Song Hi(2004) 'Molecular Dynamics Simulation Studies of the Limiting Conductances of $MgCl_2$ and $CaCl_2$ in Supercritical Water Using SPC/E Model for Water', Molecular Simulation, 30: 1, 37 — 44
To link to this Article: DOI: 10.1080/08927020310001597844
URL: http://dx.doi.org/10.1080/08927020310001597844

Molecular Simulation, VOL. 30 (1), 15 January 2004, pp. 37–44

Taylor & Francis
Taylor & Francis Group

Molecular Dynamics Simulation Studies of the Limiting Conductances of $MgCl_2$ and $CaCl_2$ in Supercritical Water Using SPC/E Model for Water

GEUN HOI GOO, GIHONG SUNG and SONG HI LEE*

Department of Chemistry, Kyungsung University, Busan 608-736, South Korea

(Received September 2002; In final form February 2003)

We report results of molecular dynamics (MD) simulations of the limiting conductances of $MgCl_2$ and $CaCl_2$ in supercritical water as a function of water density using the SPC/E model for water. The limiting conductances of Mg^{2+}, Ca^{2+} and Cl^- over the whole range of water density considered exhibits a linear dependence of the limiting conductance on the water density. In the cases of Mg^{2+} and Ca^{2+}, a solventberg picture for the behavior of small divalent cation emerges from our studies. From the view of the solventberg picture, the ion and its shell moving together as an entity interacts with the second hydration shell water molecules, and its mobility is restricted mostly by the number of the second hydration shell water which is proportional to the water density of the whole system. In the case of Cl^-, the range of water density considered in this study belongs to the higher-density region (above 0.45 g/cm^3) in which the effect of the number of hydration water molecules around ions dominated. As the water density increases, the water molecules of the first hydration shell restrict the mobility of Cl^- and the limiting conductance of Cl^- decreases nearly linearly. Significant different dependence on the water density is observed between the calculated limiting conductances of $MgCl_2$ and $CaCl_2$ at 673 K and the experimental results over the water density of 0.60–0.90 g/cm^3. Possible limitation of the extended simple point charge (SPC/E) model with regard to this difference should be pointed out and the use of a more precise model like the revised polarizable (RPOL) model is indispensable for a further MD study to gain a complete picture of the chemical circumstance around the ions.

Keywords: Molecular dynamics simulation; Limiting conductances; $MgCl_2$; $CaCl_2$

INTRODUCTION

Recently, Frantz and Marshall [1] measured the electrical conductances of $MgCl_2$ and $CaCl_2$ in dilute aqueous solutions from 25 to 600°C at pressures up to 4000 bars. Solution compositions of the salts used were between 0.001 and 0.005 molal. The results showed that in $MgCl_2$ and $CaCl_2$ solutions with compositions less than 0.005 molal the salts exist primarily as Mg^{2+}, Ca^{2+} and Cl^- ions at temperatures below 400°C and densities greater than 0.75 g/cm^3. They computed the limiting equivalent conductances in this temperature–density range. Figure 1 shows clear maxima of the limiting equivalent conductances of both $MgCl_2$ (0.001 molal) and $CaCl_2$ (0.001 molal) as a function of water density below 400°C. The maxima in the limiting equivalent conductances of $MgCl_2$ and $CaCl_2$ are located around 0.75 and 0.8 g/cm^3, respectively.

The previous two experimental results [2,3] of the limiting equivalent conductances as a function of water density in supercritical water showed two different trends: Zimmerman *et al.* [2] reported a clear change of slope from the assumed linear dependence of limiting equivalent conductances of LiCl, NaCl, NaBr and CsBr on the water density, and the other had a clear maximum in limiting equivalent conductances of NaOH reported by Ho and Palmer [3]. The clear change of the slope from the assumed linear dependence of the limiting equivalent conductance of NaCl on the water density is located around 0.45 g/cm^3 and the maximum in the limiting equivalent conductances of NaOH is located around 0.55 g/cm^3 as shown in Fig. 1.

In previous works [4,5], we reported results of molecular dynamics (MD) simulations of NaCl, LiCl, NaBr and CsBr in supercritical water aimed at

*Corresponding author. E-mail: shlee@star.ks.ac.kr

ISSN 0892-7022 print/ISSN 1029-0435 online © 2004 Taylor & Francis Ltd
DOI: 10.1080/08927020310001597844

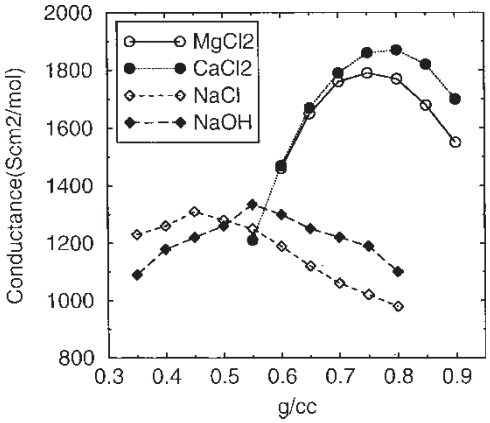

FIGURE 1 Experimental results for limiting molar conductances of $MgCl_2$ and $CaCl_2$ at infinite dilution as a function of density of supercritical water below 673 K [1], and those of NaCl and NaOH at 773 K [3].

explaining experimental observations of limiting conductance as a function of water density at supercritical state points using the extended simple point charge (SPC/E) model [6] for water and literature-derived ion–water potential parameters. We explained the experimental observations in terms of a changing balance between two competing factors—the effect of the number of hydration water molecules around ions and the interaction strength between the ions and the hydration water molecules. The number of hydration water molecules around ions was the dominating factor in the higher-density region while the interaction between the ions and the hydration water molecules dominated in the lower-density region. The competition between these two factors was evident in the residence time of water in the first hydration shell around the ions. The different effects in the lower and higher-density regimes led to different slopes for the limiting conductances as a function of water density in the two regimes.

Similar consideration of the residence time explains the dependence of ion mobility on ion size at ambient conditions, as reported in MD simulations of the mobilities of the alkali metal ions (Li^+, Na^+, K^+, Rb^+ and Cs^+) and the halides (F^-, Cl^-, Br^- and I^-) at 298 K [7–9] using the four points transferable intermolecular potential (TIP4P) [10,11] and SPC/E models [6] for water and ion–water potential parameters. The residence times of water in the hydration shells around an ion were found to decrease dramatically with its size. The classical solventberg model describes the mobility of Li^+ ion in water adequately but not those of the other ions. For the large ions, the steric effect due to large ion size and the large number of hydration water molecules restrict ionic mobility. As the size of an ion decreases, it should diffuse more easily due to the smaller steric effect and the decreasing number of the hydration water molecules. But for the small ions, the increase in the interaction between an ion and the hydrated water, reflected in the average potential energy per hydration water molecule [5], strongly decreases ionic mobility. This effect is seen in the residence time of the water in the first hydration shell around the ion.

In this paper, we extend our MD simulations of the systems to $MgCl_2$ and $CaCl_2$ in supercritical water at 673 K using the SPC/E model for water. The study for these systems is in conjunction with our previous study [12] of NaCl to delineate the effect of charge doubling. The introduction of non-additive interaction effect by the use of the revised polarized (RPOL) models [13,14] for water and ions in dilute aqueous solutions of $MgCl_2$ and $CaCl_2$ will be the next subject in our series of studies on ionic systems [4,5,7–9,12,15]. In the following section, we describe the technical details of MD simulation. We present our results in the third section and the concluding remarks in the fourth section.

MOLECULAR MODELS AND MOLECULAR DYNAMICS SIMULATION DETAILS

The SPC/E model [6] was adopted for the water molecule. All ions were represented by a point charge having a Lennard–Jones (LJ) center. The ion–oxygen σ_{io} and ε_{io} for Cl^- ion are 3.785 Å and 0.5216 kJ/mol [8,9], respectively. However, the LJ parameters for Mg^{2+} and Ca^{2+} ions are hardly found in the literature. A useful way is to deduce these parameters from Mg^{2+}-water [16] and C^{2+}-water [17] pair potentials calculated with $V_{M-O}(r)$ and $V_{M-H}(r)$ pair potentials where $M = Mg^{2+}$ and Ca^{2+}, whose derivation was based on *ab initio* calculations of different ion–water configurations. Thus, the LJ parameters used in this study for Mg^{2+} and Ca^{2+} ions are 1.91 and 2.38 Å for σ_{io}, and 147 and 81.8 kJ/mol for ε_{io}, respectively. A spherical cutoff r_c of half the simulation box length was employed for all the pair interactions. This is a simple truncation in which two molecules are considered as interacting if the distance between their centers is less than the cutoff radius r_c and the interaction is neglected if the distance is larger than r_c. This simple truncation of all interactions for water containing a single ion was shown by Perera *et al.* [18] to be comparable in accuracy to the use of Ewald summation [19] or reaction field methods [20].

The experimental critical properties of water are $T_c = 647.13$ K, $\rho_c = 0.322$ g/cm^3 and $P_c = 220.55$ bar [21] and the critical properties of SPC/E water are $T_c = 640$ K, $\rho_c = 0.29$ g/cm^3 and $P_c = 160$ bar [22]. We chose the simulation state points for the calculation of the limiting conductance of Mg^{2+}, Ca^{2+} and Cl^- ions, $T_r = T/T_c = 1.05$ (673 K) and at

the reduced densities, $\rho_r = \rho/\rho_c = 2.07$, 2.24, 2.41, 2.59, 2.76, 2.93 and 3.10, corresponding to real densities of about 0.6, 0.65, 0.7, 0.75, 0.8, 0.85 and 0.9 g/cm^3 for the SPC/E model; this spans the range of densities around 0.75–0.8 g/cm^3 where the maxima in the limiting equivalent conductances of $MgCl_2$ and $CaCl_2$ are located around 0.75–0.8 g/cm^3 [1].

We used Gaussian isokinetics [23–26] to keep the temperature of the system constant and the quaternion formulation [27,28] of the equations of rotational motion about the center of mass of the SPC/E water molecules. For the integration over time, we adopted Gear's fifth-order predictor–corrector algorithm [29,30] with a time step of 0.5×10^{-15} s (0.5 fs). Each MD simulation of a single ion system with 215 SPC/E water were carried out for Mg^{2+}, Ca^{2+} and Cl^- for 1,200,000 time steps after equilibration of 600,000 time steps. The equilibrium properties are averaged over 6 blocks of 200,000 time steps and the configurations of water molecules and an ion are stored every 10 time steps for further analysis.

The diffusion coefficient, D_i, of each ion is calculated from the mean square displacement (MSD) and from the velocity auto-correlation function (VAC) and the ion mobility is obtained by $u_i = D_i z_i e/k_B T = D_i z_i F/RT$ (Einstein relation) where k_B is the Boltzmann constant, R is the gas constant, F is the Faraday constant, z_i is the charge on the ion in units of the electronic charge e, T is the absolute temperature and $i = +$ and $-$. The limiting conductance of each ion can be calculated from

$$\lambda_i^o = u_i z_i F = D_i z_i^2 F^2/RT. \quad (1)$$

The total limiting conductance of a salt is the sum of contributions from its individual ions: $\lambda^o = \nu_+\lambda_+^o + \nu_-\lambda_-^o$, where ν_+ and ν_- are the number of cations and anions per formula unit of electrolyte (e.g. $\nu_+ = 1$ and $\nu_- = 2$ for $MgCl_2$ and $CaCl_2$).

RESULTS AND DISCUSSION

In Fig. 2, we show ion–oxygen $g_{i-O}(r)$ and ion–hydrogen $g_{i-H}(r)$ radial distribution function for Ca^{2+} ion at 673 K over the whole range of water density considered. A tall, sharp peak in $g_{i-O}(r)$ corresponding to the first solvation shell, followed by a shorter and broader second peak, is observed. The behavior of $g_{i-H}(r)$ is similar to $g_{i-O}(r)$ but much broader. The heights of the peaks for both $g_{i-O}(r)$ and $g_{i-H}(r)$ decreases with the water density. The first peak in $g_{i-O}(r)$ for Mg^{2+} ion is much higher than that for Ca^{2+} as shown in Fig. 3, which shows $g_{i-O}(r)$ and $g_{i-H}(r)$ for Mg^{2+}, Ca^{2+} and Cl^- at 673 K and a density of 0.75 g/cm^3. For Cl^- ion, the ion–oxygen $g_{i-O}(r)$ has nearly only one peak unlike in the case of

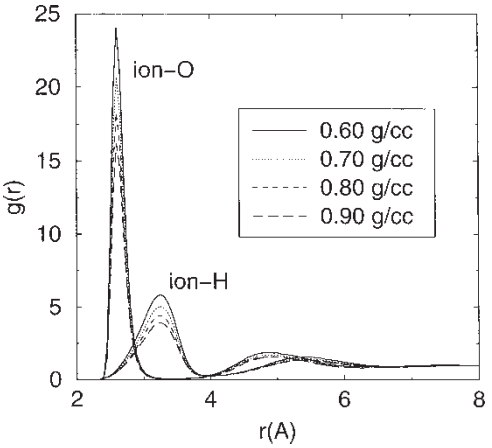

FIGURE 2 Ion–oxygen $g_{i-O}(r)$ and ion–hydrogen $g_{i-H}(r)$ for Ca^{2+} radial distribution functions ion at 673 K over the water density of 0.60–90 g/cm^3.

Mg^{2+} and Ca^{2+} (see Table I), while the ion–hydrogen $g_{i-H}(r)$ is consisted of two peaks as in the cases of Mg^{2+} and Ca^{2+}. It is also observed that the $g_{i-H}(r)$ is consisted of only one peak per hydration shell for Mg^{2+} and Ca^{2+}, but two for Cl^-.

Table I contains the positions and magnitudes of the maxima and minima of $g_{i-O}(r)$ and $g_{i-H}(r)$ radial distribution functions at 673 K over the whole range of water density considered. These values of $g_{i-O}(r)$ for Ca^{2+} at 673 K are comparable with those for Ca^{2+} at ambient temperature (298 K) [9]: 2.45 Å and 14.1 at 1st max., 3.39 Å and 0.01 at 1st min. and 4.46 Å and 1.96 at 2nd max. for r_{i-O} and g_{i-O}, respectively, even though the LJ parameters for Ca^{2+} ion–oxygen interaction are very different (3.019 Å for σ_{io} and 0.5216 kJ/mol for ε_{io}, respectively). The earlier studies using the Mg^{2+}-water [16] and Ca^{2+}-water [17] pair potential based on *ab initio* calculations also reported similar results: 2.00 Å and 19.2 at 1st max., 2.3–3.0 Å and ≈0 at 1st min. and 4.57 Å and 2.03 at

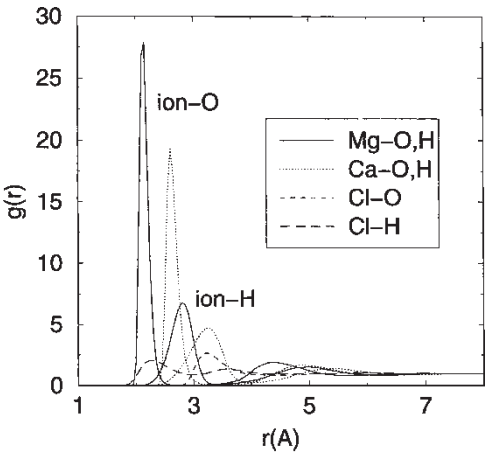

FIGURE 3 Ion–oxygen $g_{i-O}(r)$ and ion–hydrogen $g_{i-H}(r)$ radial distribution functions for Mg^{2+}, Ca^{2+} and Cl^- ions at 673 K and water density of 0.75 g/cm^3.

TABLE I Positions(A) and magnitudes at maxima and minima of $g_{i-O}(r)$ and $g_{i-H}(r)$ radial distribution functions at 673 K

		$g_{i-O}(r)$						$g_{i-H}(r)$					
		1st max.		1st min.		2nd max.		1st max.		1st min.		2nd max.	
Ion	Density (g/cm^3)	r_{i-O}	g_{i-O}	r_{i-O}	g_{i-O}	r_{i-O}	g_{i-O}	r_{i-H}	g_{i-H}	r_{i-H}	g_{i-H}	r_{i-H}	g_{i-H}
Mg^{2+}	0.60	2.1	34.2	2.8	0.05	4.4	2.2	2.8	8.4	3.4	0.1	4.9	1.7
Mg^{2+}	0.65	2.1	31.9	2.9	0.04	4.4	2.1	2.8	7.8	3.4	0.1	5.0	1.6
Mg^{2+}	0.70	2.1	29.7	2.8	0.03	4.4	2.0	2.8	7.3	3.4	0.1	5.0	1.6
Mg^{2+}	0.75	2.1	27.8	2.9	0.03	4.4	1.9	2.8	6.8	3.4	0.1	5.0	1.5
Mg^{2+}	0.80	2.1	26.1	2.9	0.03	4.4	1.8	2.8	6.4	3.4	0.1	5.0	1.5
Mg^{2+}	0.85	2.1	25.0	2.9	0.03	4.4	1.8	2.8	6.0	3.4	0.1	5.0	1.5
Mg^{2+}	0.90	2.1	23.5	2.9	0.02	4.4	1.8	2.8	5.7	3.4	0.1	4.9	1.4
Ca^{2+}	0.60	2.6	24.1	3.5	0.07	4.9	1.9	3.2	5.9	4.0	0.3	5.4	1.6
Ca^{2+}	0.65	2.6	22.4	3.5	0.07	4.9	1.8	3.2	5.4	4.0	0.3	5.4	1.5
Ca^{2+}	0.70	2.6	20.7	3.4	0.07	4.9	1.7	3.2	5.1	4.0	0.3	5.4	1.5
Ca^{2+}	0.75	2.6	19.4	3.4	0.06	4.9	1.7	3.2	4.8	4.0	0.3	5.4	1.4
Ca^{2+}	0.80	2.6	18.3	3.4	0.06	4.9	1.6	3.2	4.4	4.0	0.3	5.4	1.4
Ca^{2+}	0.85	2.6	17.1	3.4	0.06	4.8	1.6	3.2	4.2	4.0	0.3	5.4	1.4
Ca^{2+}	0.90	2.6	16.2	3.4	0.05	4.9	1.6	3.2	3.9	4.0	0.3	5.4	1.3
Cl^-	0.60	3.2	3.0	4.4	0.9	5.8	1.1	2.3	2.4	3.0	1.1	3.6	1.6
Cl^-	0.65	3.2	2.9	4.4	0.9	5.8	1.1	2.3	2.3	3.0	1.0	3.6	1.5
Cl^-	0.70	3.2	2.7	4.5	0.9	5.8	1.1	2.3	2.2	3.0	0.9	3.6	1.4
Cl^-	0.75	3.2	2.7	4.4	0.9	5.8	1.0	2.3	2.1	3.0	0.9	3.6	1.4
Cl^-	0.80	3.2	2.5	4.4	0.9	5.8	1.0	2.3	2.0	3.0	0.8	3.6	1.3
Cl^-	0.85	3.2	2.5	4.4	0.9	5.8	1.0	2.3	2.0	3.0	0.8	3.6	1.3
Cl^-	0.90	3.2	2.5	4.4	0.9	5.8	1.0	2.3	1.9	3.0	0.8	3.6	1.3

2nd max. for r_{i-O} and g_{i-O} for Mg^{2+} and 2.39 Å and 14.0 at 1st max., 3.2–3.7 Å and 0.05 at 1st min. and 4.53 Å and 2.15 at 2nd max. for r_{i-O} and g_{i-O} Ca^{2+}. No results for $g_{i-O}(r)$ and $g_{i-H}(r)$ for Mg^{2+}-water and Ca^{2+}-water systems at supercritical temperatures are reported.

We have calculated $g_{i-O}(r)$ and $g_{i-H}(r)$ for Cl^- over the water density of 0.22–0.74 g/cm^3 and at 673 K in a previous study [4] but the results are not available anymore. Comparable results, however, are available by a recent study for this system at 683 K [31] using the exactly same SPC/E potential parameters with reaction field method [20] for long-range Coulomb interactions: 3.2 Å and 2.6 at 1st max., 4.4 Å and 0.80 at 1st min. and 5.9 Å and 1.1 at 2nd max. for r_{i-O} and g_{i-O} at 0.997 g/cm^3, 3.2 Å and 5.0 at 1st max., 4.7 Å and 1.2 at 1st min. and 5.8 Å and 1.4 at 2nd max. for r_{i-O} and g_{i-O} at 0.35 g/cm^3, and 3.2 Å and 8.8 at 1st max., 4.9 Å and 1.7 at 1st min. and 5.6 Å and 2.0 at 2nd max., for r_{i-O} and g_{i-O} at 0.20 g/cm^3.

Some thermodynamic, structural and dynamic quantities have been calculated and listed in Table II. The average ion–water potential energies for Mg^{2+}, Ca^{2+} and Cl^- negatively decreases monotonically

TABLE II Average ion–water potential energy, hydration number, ion–water potential energy divided by the hydration number, and residence time of water molecules in the first hydration shell of an ion at 673 K

Ion	Density (g/cm^3)	Ion–water PE (kJ/mol)	Hydration number (n)	Ion–water (PE/n)	Residence time of water (ps)
Mg^{2+}	0.60	− 4126 ± 10	7.62 ± 0.03	− 541 ± 1	63.7 ± 6.4
Mg^{2+}	0.65	− 4145 ± 10	7.68 ± 0.04	− 540 ± 1	64.2 ± 9.3
Mg^{2+}	0.70	− 4156 ± 8	7.69 ± 0.04	− 540 ± 1	67.8 ± 8.2
Mg^{2+}	0.75	− 4160 ± 6	7.68 ± 0.02	− 542 ± 1	63.2 ± 9.2
Mg^{2+}	0.80	− 4167 ± 8	7.69 ± 0.04	− 542 ± 1	66.2 ± 9.8
Mg^{2+}	0.85	− 4188 ± 6	7.75 ± 0.04	− 540 ± 1	66.0 ± 5.7
Mg^{2+}	0.90	− 4195 ± 8	7.74 ± 0.04	− 542 ± 1	68.3 ± 4.9
Ca^{2+}	0.60	− 3326 ± 10	10.0 ± 0.1	− 333 ± 1	46.7 ± 5.1
Ca^{2+}	0.65	− 3333 ± 7	10.0 ± 0.1	− 333 ± 1	47.3 ± 6.1
Ca^{2+}	0.70	− 3341 ± 12	10.1 ± 0.2	− 331 ± 1	47.5 ± 2.9
Ca^{2+}	0.75	− 3347 ± 5	10.1 ± 0.1	− 331 ± 1	47.2 ± 5.8
Ca^{2+}	0.80	− 3356 ± 9	10.1 ± 0.1	− 332 ± 1	46.3 ± 5.5
Ca^{2+}	0.85	− 3370 ± 11	10.2 ± 0.1	− 330 ± 1	46.7 ± 4.4
Ca^{2+}	0.90	− 3385 ± 12	10.3 ± 0.1	− 329 ± 1	48.2 ± 6.2
Cl^-	0.60	− 461 ± 5	8.25 ± 0.44	− 55.9 ± 0.6	1.60 ± 0.07
Cl^-	0.65	− 464 ± 4	8.34 ± 0.33	− 55.6 ± 0.5	1.58 ± 0.09
Cl^-	0.70	− 467 ± 3	8.45 ± 0.44	− 55.3 ± 0.3	1.56 ± 0.08
Cl^-	0.75	− 472 ± 4	8.56 ± 0.57	− 55.1 ± 0.4	1.55 ± 0.05
Cl^-	0.80	− 475 ± 4	8.90 ± 0.73	− 53.4 ± 0.4	1.58 ± 0.06
Cl^-	0.85	− 478 ± 4	9.16 ± 0.55	− 52.2 ± 0.4	1.62 ± 0.06
Cl^-	0.90	− 483 ± 3	9.53 ± 0.66	− 50.7 ± 0.3	1.66 ± 0.07

with decreasing water density as was observed in all the MD simulations for ion–water systems [4,5,12,15]. This is easily understood from the point of view that the number of water around an ion is decreased as seen in the hydration number.

The hydration number n is found by integrating the ion–oxygen radial distribution function $g_{i-O}(r)$ from the inner to the outer boundary of the first solvation shell:

$$n = 4\pi\rho\int_0^{r_{min}} g_{io}(r)r^2\,dr \tag{2}$$

where ρ is the number density of bulk water and r_{min} is the point at which the first minimum in $g_{i-O}(r)$ occurs. Table II lists the hydration number of water in the first solvation shell around Mg^{2+}, Ca^{2+} and Cl^- ions. The hydration numbers reported by other MD studies are 6.0 [16] around Mg^{2+} at 300 K, and 9.2 [17] at 300 K and 7.9 [9] at 298 K around Ca^{2+}. The large difference in the hydration number of the two results for Ca^{2+} seems to originate from the different ion–water potential forms used. For Cl^- at a supercritical temperature of 683 K, 10 at 0.997 g/cm^3, 8 at 0.35 g/cm^3 and 7 at 0.20 g/cm^3 [31] are reported which are comparable with our results. Our previous results for the hydration number for Cl^- over the water density of 0.22–0.74 g/cm^3 and at 673 K [4] were in good agreement with the current results over the water density of 0.60–0.90 g/cm^3 and at 673 K. The changes of the hydration numbers for Mg^{2+} and Ca^{2+} over the water density of 0.60–0.90 g/cm^3 are 0.1 and 0.3, respectively, and thus the hydration numbers for Mg^{2+} and Ca^{2+} are nearly constant when compared with the change of the hydration number for Cl^- (1.3) over the same range of water density. This is probably due to the strong Coulomb interaction of the divalent ion with the hydration water molecules and so the hydration number is non-sensitive to the water density, unlike in the cases of monovalent ions. The hydration number for Cl^- over the water density of 0.60–90 g/cm^3 decreases slightly more rapidly with decreasing water density than that of 0.22–0.74 g/cm^3 [4]. It decreases rapidly up to 0.75 g/cm^3 and then slows down as the same rate as that of 0.48–0.74 g/cm^3 [4].

The potential energy per hydration water molecule, defined as the average ion–water potential energy divided by the hydration number, for Mg^{2+}, Ca^{2+} and Cl^- ions is also listed in Table II. In the case of Mg^{2+} and Ca^{2+}, these energies are almost constant over the whole range of water density. This is largely due to the small changes in the average ion–water potential energies and the hydration numbers. The small change in the energetics of Mg^{2+} and Ca^{2+} and the structure of water around these ions suggests that the chemical circumstances around these ions are almost invariable over the whole range of water density considered, and this is again mainly due to the strong divalent ion–water interaction unlike in the cases of monovalent ions. The same kind of behavior for different ions (Na^{2+} and Cl^{2-}) over the water density of 0.48–0.74 g/cm^3 was already seen in a previous study [14]. The potential energy per hydration water for Cl^- over the water density of 0.60–90 g/cm^3 show the same trend as the hydration number: it negatively increases rapidly with decreasing water density up to 0.75 g/cm^3 and then slows down as the same rate as that of 0.48–0.74 g/cm^3 [4].

The residence time correlation function is defined by [7,8]

$$R(r,t) = \frac{1}{N_r}\sum_{i=1}^{N_r}[\theta_i(r,t)\theta_i(r,0)] \tag{3}$$

where $\theta_i(r,t)$ is the Heaviside unit function, which is 1 if a water molecule i is within a spherical region of radius r within the first hydration shell of the ion and 0 otherwise and N_r is the average number of water molecules in this region r at $t = 0$. The characteristic decay time (residence time), τ, is obtained by fitting the time correlation function to an exponential decay $\langle R(r,t)\rangle \cong \exp(-t/\tau)$, which is useful particularly when τ is large. The residence times of water within the first hydration shell around Mg^{2+}, Ca^{2+} and Cl^- ions are listed in Table II. The residence times for Mg^{2+} and Ca^{2+} over the whole range of water density considered are much larger than those of monovalent ions—Na^+ (1.7–2.4), Cl^- (1.5–1.9) [4], Cs^+ (1.6–2.1) and Br^- (1.7–2.1) [5]—by an order of magnitude due to the strong Coulomb interaction of the divalent ions with the hydration water molecules. However, the changes in these numbers for the water density of 0.22–0.74 g/cm^3 are very small (5.1/65.6 and 1.9/47.1 for Mg^{2+} and Ca^{2+}, respectively) when compared with those for Na^+ (0.8/2.1), Cl^- (1.8/7.7) [4], Cs^+ (2.5/7.5) and Br^- (2.2/8.4) [5] for the water density of 0.60–90 g/cm^3 in which the numerator is the difference in the numbers and the denominator is the average of the numbers. The picture of the behavior of small divalent cations that emerges from our studies is that of a hydrated solventberg ion: the ion and its shell move together as an entity bestowing a large effective radius on the ion and a small mobility. The first system described by classical solventberg model was the mobility of Li^+ ion in water at ambient temperature [7,8] but not at supercritical temperatures [5]. The solventberg picture for Ca^{2+} was also seen at ambient temperature [9]. The residence time for Cl^- decreases with decreasing water density up to 0.75 g/cm^3 and then increases as the same rate as that of 0.48–0.74 g/cm^3 [4].

The diffusion coefficients D_i of Mg^{2+}, Ca^{2+} and Cl^-, calculated from the MSDs and from the VACs, are listed in Table III. The limiting conductances λ°

TABLE III Diffusion coefficient D_i and molar conductance λ_i° of Mg^{2+}, Ca^{2+} and Cl^- at infinite dilution in supercritical water at 673 K calculated from mean square displacement (MSD) and velocity autocorrelation function (VAC)

		$D_i(\times 10^{-5} cm^2/s)$		$\lambda_i^\circ(\times Scm^2/mol)$	
Ion	*Density (g/cm^3)*	*MSD*	*VAC*	*MSD*	*VAC*
Mg^{2+}	0.60	8.96 ± 0.09	9.05 ± 0.10	596 ± 57	602 ± 66
Mg^{2+}	0.65	8.48 ± 0.13	8.52 ± 0.14	564 ± 87	567 ± 95
Mg^{2+}	0.70	8.38 ± 0.10	8.31 ± 0.10	557 ± 65	553 ± 66
Mg^{2+}	0.75	7.64 ± 0.10	7.63 ± 0.11	508 ± 65	506 ± 72
Mg^{2+}	0.80	7.25 ± 0.13	7.30 ± 0.13	482 ± 85	486 ± 85
Mg^{2+}	0.85	6.88 ± 0.10	6.95 ± 0.11	458 ± 67	462 ± 75
Mg^{2+}	0.90	5.94 ± 0.06	5.89 ± 0.07	395 ± 41	392 ± 43
Ca^{2+}	0.60	11.1 ± 0.1	11.5 ± 0.1	738 ± 60	765 ± 60
Ca^{2+}	0.65	10.5 ± 0.1	10.6 ± 0.1	699 ± 67	705 ± 60
Ca^{2+}	0.70	10.1 ± 0.1	10.2 ± 0.1	672 ± 93	679 ± 93
Ca^{2+}	0.75	9.63 ± 0.10	9.62 ± 0.11	641 ± 68	640 ± 75
Ca^{2+}	0.80	8.68 ± 0.11	8.58 ± 0.12	577 ± 75	571 ± 83
Ca^{2+}	0.85	7.69 ± 0.11	7.82 ± 0.12	512 ± 74	520 ± 83
Ca^{2+}	0.90	7.23 ± 0.13	7.17 ± 0.14	481 ± 85	477 ± 92
Cl^-	0.60	38.6 ± 0.5	38.6 ± 0.5	642 ± 75	642 ± 75
Cl^-	0.65	37.3 ± 0.4	37.7 ± 0.4	620 ± 72	627 ± 70
Cl^-	0.70	35.2 ± 0.5	35.6 ± 0.5	585 ± 77	592 ± 85
Cl^-	0.75	33.2 ± 0.5	33.3 ± 0.5	552 ± 87	554 ± 90
Cl^-	0.80	30.9 ± 0.5	30.9 ± 0.5	514 ± 78	514 ± 82
Cl^-	0.85	27.4 ± 0.4	27.2 ± 0.4	456 ± 58	452 ± 62
Cl^-	0.90	25.4 ± 0.5	25.3 ± 0.5	422 ± 87	421 ± 88

determined from these diffusion coefficients are also listed in the same table and those from MSD only are plotted in Fig. 4. The limiting conductances of Mg^{2+}, Ca^{2+} and Cl^- over the whole range of water density considered exhibits a linear dependence on the water density.

The monotonous decrement of the limiting conductance of divalent ions with water density was already seen for Na^{2+} and Cl^{2-} over the water density of 0.48–0.74 g/cm^3 in a previous study [14]. A possible explanation for this may be the strong Coulomb interaction of the divalent ions with the hydration water molecules: the average ion–water potential energies for Mg^{2+} and Ca^{2+} ions increases nearly linearly and very slowly with decreasing water density but the potential energy per hydration water are almost constant over the water density of 0.60–90 g/cm^3 as discussed above. Thus, between two important competing factors in the explanation of the limiting conductances of LiCl, NaCl, NaBr and CsBr in supercritical water at 673 K [4,5], the effect of the ion–water interaction strength becomes non-factor against the other effect, which is that of the number of hydration water molecules around ions. From the view of the solventberg picture of these ions, the ion and its shell moving together as an entity interacts with the second hydration shell water which is proportional to the water density of the whole system.

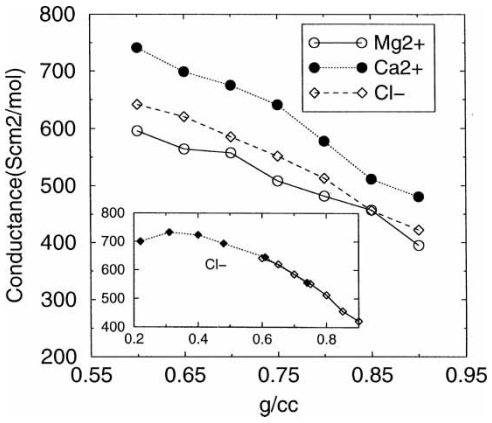

FIGURE 4 Limiting molar conductances of Mg^{2+}, Ca^{2+} and Cl^- at infinite dilution as a function of density of supercritical water at 673 K obtained from MSD's. The inset shows limiting molar conductances of Cl^- at the lower densities of water (◆) obtained from the previous study [4].

The monotonous decrement of the limiting conductance of Cl^- over the whole range of water density (0.60–0.90 g/cm^3) is consistent with those over the water density of 0.22–0.74 g/cm^3 in the previous study [4] as shown in the inset of Fig. 4. The range of water density considered in this study belongs to the higher-density region (above 0.45 g/cm^3) in which the effect of the number of hydration water molecules around ions dominated [4]. As the water density increases, the water molecules of the first hydration shell restrict the mobility of Cl^- and the limiting conductance of Cl^- decreases nearly linearly.

The limiting conductances of $MgCl_2$ and $CaCl_2$ calculated from those of the individual ions by $\lambda^\circ = \lambda_{2+}^\circ + 2\lambda^\circ$ are compared with the experimental results in Fig. 5. The experimental results show clear maxima of the limiting conductances of both $MgCl_2$ and $CaCl_2$ as a function of water density with the maxima around 0.75 and 0.8 g/cm^3, respectively, while the MD simulation results exhibits a linear

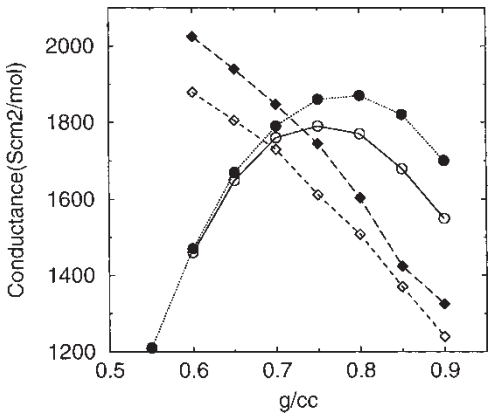

FIGURE 5 Comparison of the limiting molar conductances of $MgCl_2$ and $CaCl_2$ at infinite dilution as a function of density of supercritical water at 673 K obtained from MSD's with the experimental results [1].

dependence of the limiting conductance on the water density. It is fortunate enough that the calculated limiting conductances of $MgCl_2$ and $CaCl_2$ give the same range of magnitude as the experimental results over the whole range of water density considered. As a matter of course, the monotonous decrement of the limiting conductance of $MgCl_2$ and $CaCl_2$ over the whole range of water density (0.60–0.90 g/cm^3) originates from those of Mg^{2+}, Ca^{2+} and Cl^- which was fully discussed above.

The same kind of behavior for linear dependence for the limiting conductance on the water density was already seen in the limiting conductance of Li^+ in the previous MD studies [5,15]: good agreement with limiting conductance experimental results at supercritical conditions was found for NaCl, NaBr and CsBr except LiCl [4,5]. Since the limiting conductance of other chloride salt (NaCl) was well predicted, the poor result for LiCl was clearly a reflection of the poor prediction for that of Li^+. The limiting conductances of Li^+ over the water density of 0.22–0.74 g/cm^3 calculated from MD simulations underestimated the experimental results [2] and exhibited almost linear dependence for the limiting conductance on the water density. The hydration number for Li^+ was nearly unchanged over the water density considered, and the interaction between the ions and the hydration water in the lower-density region was almost a non-factor since the potential energy per hydration water molecule monotonically decreased with decreasing water density. The slope of the residence time (versus water density) for Li^+ in the lower density region was smaller than in the higher-density region.

The overall situation for Mg^{2+} (Ca^{2+}) and Li^+ is very similar to the point of view that the potential energy per hydration water is non-factor in the lower density region, but there exists a clear difference for the non-factor of the ion-factor of the ion–water interaction energy: in the case of Li^+, the potential energy per hydration water molecule in the cases of Na^+, Cs^+, Cl^- and Br^- [4,5] while the chemical circumstance of Mg^{2+} and Ca^{2+} is described by the picture of a hydrated solventberg ion—the ion and its shell move together as an entity due to the strong Coulomb interaction of the divalent ion with the hydration water molecules over the whole range of water density considered.

CONCLUDING REMARKS

In this study, we have extended our MD simulations of the systems to Mg^{2+}, Ca^{2+} and Cl^- in supercritical water 673 K using the SPC/E model for water to delineate the behavior of the divalent cations. The limiting conductances of Mg^{2+}, Ca^{2+} and Cl^- over the whole range of water density considered exhibits a linear dependence on the water density. In the cases of Mg^{2+} and Ca^{2+}, the hydration number of water in the first solvation shell around the ion increases with water density but are almost constant over the water density 0.60–0.90 g/cm^3, and the potential energy per hydration water molecule is very strong but nearly non-factor on the water density. The residence time for these divalent cations over the whole range of water density considered are much larger than those of monovalent ions by an order of magnitude due to the strong Coulomb interaction of the divalent ions with the hydration water molecules, but the changes in the residence times for the given water density are very small when compared with those for the monovalent ions. The picture of the behavior of small divalent cations that emerges from our studies is that of a hydrated solventberg ion. From the view of the solventberg picture, the ion and its shell moving together as an entity interacts with the second hydration shell water molecules, and its mobility is restricted mostly by the number of the second hydration shell water which is proportional to the water density of the whole system. The overall situation for Mg^{2+} (Ca^{2+}) and Li^+ is very similar from the point of view that the ion–water interaction energy is non-factor in the lower density region, but in the case of Li^+, the potential energy per hydration water molecule in the lower density region is weaker than that in the higher density region unlike in the cases of Na^+, Cs^+, Cl^- and Br^- [4,5].

In the case of Cl^-, the range of water density considered in this study belongs to the higher-density region (above 0.45 g/cm^3) in which the effect of the number of hydration water molecules around ions dominated. As the water density increases, the water molecules of the first hydration shell restrict the mobility of Cl^- and the limiting conductance of Cl^- decreases nearly linearly.

While it is fortunate enough that the calculated limiting conductances of $MgCl_2$ and $CaCl_2$ give

the same range of magnitude as the experimental results at 673 K over the water density of 0.60–0.90 g/cm^3, significant different dependence on the water density is observed between the calculated and the experimental results. Possible limitation of the SPC/E model with regard to this difference should be pointed out. To gain a better limiting conductances of $MgCl_2$ and $CaCl_2$ and a more complete picture of the chemical circumstance around the ions, we are extending our MD study to the use of the revised polarizable (RPOL) model [13,14].

Acknowledgements

This research was supported by the Provincial University Support Research Fund of the Korea Science and Engineering Foundation (KOSEF), 2000. S.H. Lee thanks the Tongmyung University of Information Technology for access to its IBM SP/2 computer.

References

[1] Frantz, J.D. and Marshall, W.L. (1982) "Electrical conductances and ionization constants of calcium chloride and magnesium chloride in aqueous solutions at temperatures to 600°C and pressures to 400 bars", *American Journal of Science* **282**, 1666.

[2] Zimmerman, G.H., Gruszkiewicz, M.S. and Wood, R.H. (1995) "New apparatus for conductance measurements at high temperatures: conductance of aqueous solutions of LiCl, NaCl, NaBr, and CsBr at 28 MPa and water densities for 700 to 260 kg m^{-3n}", *J. Phys. Chem.* **99**, 11612.

[3] Ho, P.C. and Palmer, D.A. (1996) "Ion association of dilute aqueous sodium hydroxide solutions to 600°C and 300 MPa by conductance measurements", *J. Solution. Chem.* **25**, 711.

[4] Lee, S.H., Cummings, P.T., Simonson, J.M. and Mesmer, R.E. (1998) "Molecular dynamics simulation of the limiting conductance of NaCl in supercritical water", *Chem. Phys. Lett.* **293**, 289.

[5] Lee, S.H. and Cummings, P.T. (2000) "Molecular dynamics simulation of the limiting conductance of LiCl, BaBr, and CsBr in supercritical water", *J. Chem. Phys.* **112**, 864.

[6] Berendsen, H.J., Grigera, C.J.R. and Straatsma, T.P. (1987) "The missing term in effective pair potentials", *Phys. Chem.* **91**, 6269.

[7] Lee, S.H. and Rasaiah, J.C. (1994) "Molecular dynamics simulation of ionic mobility. I. Alkali metal cations in water at 25°C", *J. Chem. Phys.* **101**, 6964.

[8] Lee, S.H. and Rasaiah, J.C. (1996) "Molecular dynamics simulation of ionic mobility. 2. Alkali metal and halide ions using the SPC/E model for water at 25°C", *J. Phys. Chem.* **100**, 1420.

[9] Koneshan, S., Rasaiah, J.C., Lynden-Bell, R.M. and Lee, S.H. (1998) "Solvent structure, dynamics, and ion mobility in aqueous solutions at 25°C", *J. Phys. Chem. B.* **102**, 4193.

[10] Jorgensen, W.L. (1982) "Revised TIPS model for simulations of liquid water and aqueous solutions", *J. Chem. Phys.* **77**, 4156.

[11] Jorgensen, W.L. and Maura, J.D. (1985) "Temperature and size dependence for Monte Carlo simulations of TIP4P water", *Mol. Phys.* **56**, 1381.

[12] Lee, S.H. and Cummings, P.T. (2001) "Molecular dynamics simulation of the limiting conductance for Na^{2+}, Cl^{2-}, Na^0, and Cl^0 in supercritical water", *Mol. Sim.* **27**, 199.

[13] Caldwell, J., Dang, L.X. and Kollman, P.A. (1990) "Implementation of nonadditive intermolecular potentials by use of molecular dynamics: development of a water–water potential and water–ion cluster interactions", *J. Am. Chem. Soc.* **112**, 9144.

[14] Dang, L.X., Rice, J.E., Caldwell, J. and Kollman, P.A. (1991) "Ion solvation in polarizable water: molecular dynamics simulations", *J. Am. Chem. Soc.* **113**, 2481.

[15] Lee, S.H. (2002) "Molecular dynamics simulation of the limiting conductance of Li^+ ion in supercritical water using polarizable models", *Mol. Sim.*, **29**, 211.

[16] Dietz, W., Riede, W.O. and Heinzinger, K. (1982) "Molecular dynamics simulation of an aqueous $MgCl_2$ solution. Structural results", *Z. Naturforsch.* **37a**, 1038.

[17] Probst, M.M., Radnai, T., Heinzinger, Z., Bopp, P. and Rode, B.M. (1985) "Molecular dynamics and X-ray investigation of an aqueous $CaCl_2$ solution", *J. Phys. Chem.* **89**, 753.

[18] Perera, L., Essmann, U. and Berkowitz, M.L. (1995) "Effect of the treatment of long-range forces on the dynamics of ions in aqueous solutions", *J. Chem. Phys.* **102**, 450.

[19] De Leeuw, S.W., Perram, J.W. and Smith, E.R. (1980) "Simulation of electrostatic systems in periodic boundary conditions. I. Lattice sums and dielectric constant", *Proc. R. Soc. Lond.* **A373**, 27.

[20] Barker, J.A. and Watts, R.O. (1973) "Monte Carlo studies of the dielectric properties of water-like models", *Mol. Phys.* **26**, 789.

[21] Reid, R.C., Prausnitz, J.M. and Sherwood, T.K. (1977) *The properties of Liquids and Gases* (McGraw-Hill, New York).

[22] Guissani, Y. and Guillot, B. (1993) "A computer simulation study of the liquid–vapor coexistence curve of water", *J. Chem. Phys.* **98**, 8221.

[23] Simmons, A.D. and Cummings, P.T. (1986) "Non-equilibrium molecular dynamics simulation of dense fluid methane", *Chem. Phys. Lett.* **129**, 92.

[24] Hoover, W.G., Ladd, A.J.C. and Moran, B. (1982) "High strain rate plastic flow studied via nonequilibrium molecular dynamics", *Phys. Rec. Lett.* **48**, 1818.

[25] Evans, D.J. (1983) "Computer experiment for non-linear thermodynamics of Couette flow", *J. Chem. Phys.* **78**, 3297.

[26] Evans, D.J., Hoover, W.G., Failor, B.H., Moran, B. and Ladd, A.J.C. (1983) "Nonequilibrium molecular dynamics via Gauss's principle of least constraint", *Phys. Rev. A* **28**, 1016.

[27] Evans, D.J. (1977) "On the representation of orientation space", *Mol. Phys.* **34**, 317.

[28] Evans, D.J. and Murad, S. (1977) "Singularity free algorithm for molecular dynamics rigid polyatomics", *Mol. Phys.* **34**, 327.

[29] Gear, C.W. (1971) *Numerical Initial Value Problems in Ordinary Differential Equation* (Prentice-Hall, Englewood Cliffs, NJ).

[30] Evans, D.J. and Morriss, G.P. (1984) "Non-Newtonian molecular dynamics", *Comput. Phys. Rep.* **1**, 297.

[31] Rasaiah, J.C., Noworyta, J.P. and Koneshan, S. (2000) "Structure of aqueous solutions of ions and netural solutes at infinite dilution at a supercritical temperature of 683 K", *J. Am. Chem. Soc.* **122**, 11182.